

# Magnetic susceptibility study of hydrated and non-hydrated $\text{Na}_x\text{CoO}_2 \cdot y\text{H}_2\text{O}$ single crystals

F. C. Chou<sup>1</sup>, J. H. Cho<sup>1,2,\*</sup> and Y. S. Lee<sup>1,2</sup>

<sup>1</sup>*Center for Materials Science and Engineering,  
Massachusetts Institute of Technology*

and

<sup>2</sup>*Department of Physics, Massachusetts Institute of Technology*

(Dated: November 1, 2018)

We have measured the magnetic susceptibility of single crystal samples of non-hydrated  $\text{Na}_x\text{CoO}_2$  ( $x \simeq 0.75, 0.67, 0.5, 0.3$ ) and hydrated  $\text{Na}_{0.3}\text{CoO}_2 \cdot y\text{H}_2\text{O}$  ( $y \simeq 0, 0.6, 1.3$ ). Our measurements reveal considerable anisotropy between the susceptibilities with  $H \parallel c$  and  $H \parallel ab$ . The derived anisotropic  $g$ -factor ratio ( $g_{ab}/g_c$ ) decreases significantly as the composition is changed from the Curie-Weiss metal with  $x = 0.75$  to the paramagnetic metal with  $x = 0.3$ . Fully hydrated  $\text{Na}_{0.3}\text{CoO}_2 \cdot 1.3\text{H}_2\text{O}$  samples have a larger susceptibility than non-hydrated  $\text{Na}_{0.3}\text{CoO}_2$  samples, as well as a higher degree of anisotropy. In addition, the fully hydrated compound contains a small additional fraction of anisotropic localized spins.

PACS numbers: 74.25.Ha, 74.70.Dd, 75.20.Hr, 75.30.Gw, 75.30.Cr

## I. INTRODUCTION

The discovery of superconductivity below  $T \sim 4.5$  K in  $\text{Na}_{0.3}\text{CoO}_2 \cdot 1.4\text{H}_2\text{O}$  has engendered much interest in the family of  $\text{Na}_x\text{CoO}_2 \cdot y\text{H}_2\text{O}$  compounds.<sup>1</sup> The non-hydrated compound  $\text{Na}_x\text{CoO}_2$  with  $x \simeq 0.65 - 0.75$  has an anomalously large thermoelectric power.<sup>2</sup> Measurements in applied magnetic fields indicate that spin entropy plays an important role in the enhanced thermopower in  $\text{Na}_{0.68}\text{CoO}_2$ .<sup>3</sup> Further work has revealed that the  $\text{Na}_x\text{CoO}_2$  material crosses over from a Curie-Weiss metal ( $x > 0.5$ ) to a paramagnetic metal ( $x < 0.5$ ), separated by a charge-ordered insulator at  $x = 0.5$ .<sup>4</sup> Based on density-functional calculations, weak itinerant ferromagnetic fluctuations have been suggested to compete with weak antiferromagnetism for  $x = 0.3$  to  $x = 0.7$ .<sup>5</sup> Much recent research has focused on understanding the mechanism for superconductivity in the new hydrated superconductor. Further progress can be made by examining the bulk properties of  $\text{Na}_x\text{CoO}_2 \cdot y\text{H}_2\text{O}$  as a function of  $x$  and  $y$  in order to elucidate the intriguing physics found on the phase diagram.

In this paper, we present a systematic study of the magnetic susceptibility of  $\text{Na}_x\text{CoO}_2 \cdot y\text{H}_2\text{O}$  (with  $x \simeq 0.75, 0.67, 0.5, 0.3$  and  $y \simeq 0, 0.6, 1.3$ ) using single-crystal samples produced by an electrochemical de-intercalation method.<sup>6,7</sup> Our results show that the susceptibilities of our crystals are consistent with the behavior reported in powder samples prepared differently via chemical  $\text{Br}_2$  de-intercalation. In addition, our studies reveal that the susceptibility is clearly anisotropic. We further report how the susceptibility changes as a function of both Na and  $\text{H}_2\text{O}$  content. The paper is arranged as follows: Section II contains experimental details and initial sample characterization. Section III contains the results of our susceptibility measurements, along with analysis of our data. A discussion of our results and conclusions are in Section IV.

## II. EXPERIMENTAL

Single crystals of  $\text{Na}_{0.75}\text{CoO}_2$  were grown using the floating-zone technique. After an additional electrochemical de-intercalation procedure, samples were produced with the final Na concentrations of  $x = 0.75, 0.67, 0.5$  and  $0.3$ , as confirmed by Electron Microprobe Analysis. Details of the crystal growth process, electrochemical de-intercalation, and characterization of the resulting samples are discussed in depth in Ref. [7]. Powder neutron diffraction on a crushed single crystal of  $\text{Na}_{0.75}\text{CoO}_2$  grown under similar conditions as the samples presented here indicates that the crystalline boule consists of a single structural phase.<sup>8</sup> A crystal of  $\text{Na}_{0.7}\text{CoO}_2$  was grown using the flux method. The crystal was obtained from a melt prepared from powder mixtures of  $\text{Na}_{0.75}\text{CoO}_2 + 4\text{NaCl} + 4\text{Na}_2\text{CO}_3 + \text{B}_2\text{O}_3$  which was slowly cooled from  $920^\circ\text{C}$  to  $820^\circ\text{C}$  at a rate of  $-1^\circ\text{C/hr}$ .

A fully hydrated  $\text{Na}_{0.3}\text{CoO}_2 \cdot 1.3\text{H}_2\text{O}$  crystal was prepared by enclosing a non-hydrated  $\text{Na}_{0.3}\text{CoO}_2$  crystal within a water vapor saturated environment for  $\sim 4$  months. After this period of hydration, the crystal consisted of a single phase with a  $c$ -axis lattice constant of  $19.56(8)$  Å and with a superconducting transition temperature near  $\sim 4.2$  K. Partially hydrated  $\text{Na}_{0.3}\text{CoO}_2 \cdot 0.6\text{H}_2\text{O}$  samples and a fully dehydrated  $\text{Na}_{0.3}\text{CoO}_2$  samples were obtained by driving water out by annealing at temperatures of  $120^\circ\text{C}$  and  $220^\circ\text{C}$ , respectively, for 15 hours. Except for a small fraction of a  $\text{Co}_3\text{O}_4$  impurity phase generated in the fully dehydrated crystal, the partially hydrated and fully dehydrated phases have  $c$ -axis lattice constants of  $13.74(3)$  Å and  $11.11(5)$  Å, respectively, which are in agreement with previously reported values of  $\text{Na}_{0.3}\text{CoO}_2 \cdot 0.6\text{H}_2\text{O}$  and  $\text{Na}_{0.3}\text{CoO}_2$ .<sup>9</sup> In principle, the fully dehydrated (FD) phase should be identical to the original non-hydrated phase. Powder x-ray diffraction results confirm that the two phases share the same primary powder peaks; however, the FD sample contains

a somewhat higher degree of defects which we will discuss further below.

Measurements of the magnetic susceptibility were performed using a Quantum Design MPMS-XL SQUID magnetometer. The typical size of the crystals used in these measurements were  $4 \times 3 \times 1 \text{ mm}^3$  with mass  $\sim 50 \text{ mg}$ . These pieces were easily cleaved from the larger floating-zone boule with the larger surface area corresponding to the  $ab$ -plane. All data were measured under a magnetic field of 1 Tesla through both zero cooled and zero-field cooled sequences. Slightly hysteretic behavior was observed for the  $x = 0.75$  sample near temperatures of  $\sim 22 \text{ K}$  and  $\sim 320 \text{ K}$ , consistent with previous observations.<sup>10,11</sup> Since the focus of this paper is not on the hysteretic behavior, all of the data presented are based on the zero-field cooled results. A background correction to the susceptibility has been made on the crystals with  $x = 0.67$  and  $0.3$ . The source of this background is likely due to a small amount of CoO impurities (about a 7 % mass fraction) imbedded between the grain boundaries of the particular starting boule of  $\text{Na}_{0.75}\text{CoO}_2$ . The CoO correction was implemented as to minimize the contribution from the antiferromagnetic transition ( $T_N \sim 290 \text{ K}$ ) of CoO, while maintaining the same magnitude of the susceptibility as a powder sample of the same stoichiometry.<sup>7</sup> No correction was applied to the  $\text{Na}_{0.75}\text{CoO}_2$  and  $\text{Na}_{0.5}\text{CoO}_2$  crystals, where no anomaly at  $T \sim 290 \text{ K}$  is found and the powder averaged data agrees with the data from stoichiometric polycrystalline samples. We note, however, there is a broad maximum near  $\sim 275 \text{ K}$  for the  $\text{Na}_{0.67}\text{CoO}_2$  crystal, which may be intrinsic, as this is also reported by others.<sup>10</sup>

### III. RESULTS AND ANALYSIS

#### 1. Magnetic susceptibility of non-hydrated $\text{Na}_x\text{CoO}_2$

Our magnetic susceptibility data for  $\text{Na}_x\text{CoO}_2$  ( $x = 0.3, 0.5, 0.67$ , and  $0.75$ ) are shown in Fig. 1, where a magnetic field of 1 Tesla was applied parallel to the  $ab$ - and  $c$ - directions. Curie-Weiss-like behavior is observed for  $x > 0.5$ , but samples with  $x < 0.5$  show a monotonic increase of  $\chi$  with increasing temperature. Our results, when powder-averaged, agree with the published powder measurements on samples prepared using chemical  $\text{Br}_2$  de-intercalation.<sup>4</sup> For example, the sample with  $x = 0.5$  shows anomalies in the susceptibility at  $T \sim 88 \text{ K}$  and  $\sim 53 \text{ K}$ , consistent with that reported by Foo et.al.<sup>4</sup> Moreover, we find that the anomaly at  $88 \text{ K}$  is only apparent in  $\chi_{ab}$ .

These measurements on single crystals yield additional information on the spin anisotropy for the various compositions. In Fig. 2, plots of  $\chi_{ab}$  versus  $\chi_c$  are shown for all crystals for temperatures between 50 and 250 K, where  $T$  is an implicit parameter. The  $\chi_{ab}$  versus  $\chi_c$  curve shows a remarkably linear relationship for all  $x$ . This linear relationship holds both for samples with Curie-Weiss be-

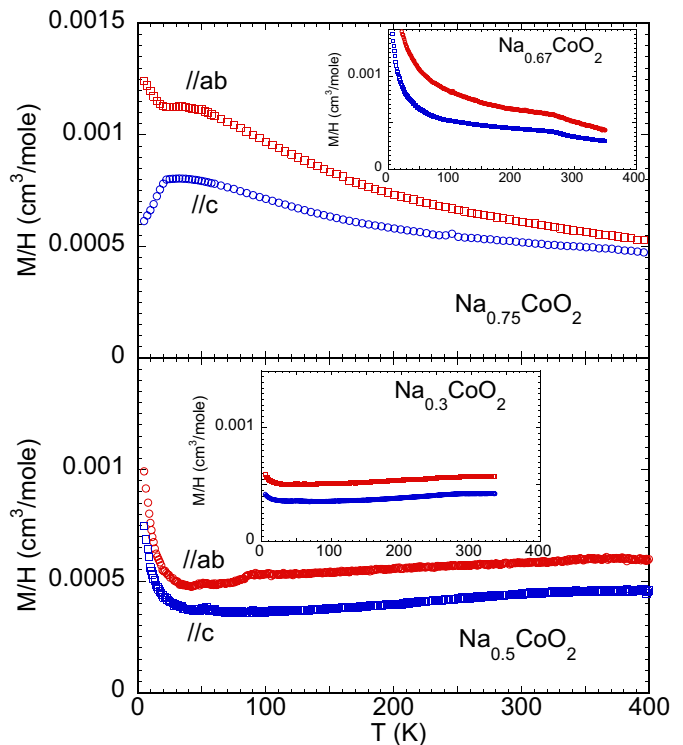


FIG. 1: (color online) Magnetic susceptibilities of  $\text{Na}_x\text{CoO}_2$  ( $x = 0.75, 0.67, 0.5$ , and  $0.3$ ) under a magnetic field of 1 Tesla. The red and blue symbols are for the magnetic field applied along the  $ab$ - and  $c$ - directions, respectively.

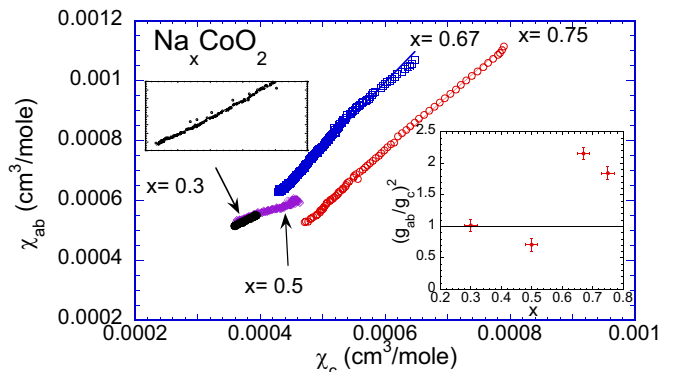


FIG. 2: (color online)  $\chi_{ab}$  versus  $\chi_c$  for  $\text{Na}_x\text{CoO}_2$  with  $x = 0.75, 0.67, 0.5$  and  $0.3$ . The inset shows the fitted slope which corresponds to  $(g_{ab}/g_c)^2$  as described in the text.

havior ( $x > 0.5$ ) and for samples with  $\chi$  increasing with increasing  $T$  ( $x < 0.5$ ), albeit with different magnitudes of the slope.

One way to parameterize this behavior for all of our samples is with the following analysis. This analysis allows us to extract information from the slopes of the curves in Fig. 2, without assuming a specific temperature-dependence of  $\chi$ . The measured susceptibility is composed of a temperature-independent contribution  $\chi_0$

TABLE I: Curie-Weiss fitting parameters for  $\text{Na}_x\text{CoO}_2$ 

		$x=0.75$	$x=0.70^a$	$x=0.67$
$\parallel ab$	$\chi_o$	.000187	.000268	.000375
$\parallel ab$	$C$	.181	.145	.0677
$\parallel ab$	$\theta$	-130	-103	-46.9
$\parallel c$	$\chi_o$	.000326	.000223	.000358
$\parallel c$	$C$	.0751	.0665	.0183
$\parallel c$	$\theta$	-93	-64.5	-12.0
Powder	$\chi_o$	.000231	.000267	.000356
Powder	$C$	.147	.112	.0554
Powder	$\theta$	-125	-87.8	-46.9

<sup>a</sup>flux grown

(which includes the Van Vleck paramagnetism and the core diamagnetism) and a temperature-dependent term  $\chi_e(T)$  (which represents contributions from either localized spins or the spin response of delocalized electrons):  $\chi_{ab,c}(T) = \chi_o^{ab,c} + \chi_e^{ab,c}(T)$ . We then write the temperature-dependent term in the form  $\chi_e^{ab,c}(T) = (g_{ab,c})^2 f(T)$ , which assumes that the anisotropy of the spin susceptibility  $\chi_e$  results from an anisotropic  $g$ -factor. Note that the  $g$ -factor for localized spins is related to the spin-orbit coupling, and the effective  $g$ -factor for delocalized electrons is related to the coupling between the applied field and the total angular momentum of the system. This leads to the following relation between  $\chi_{ab}(T)$  and  $\chi_c(T)$ :

$$\chi_{ab}(T) = (g_{ab}/g_c)^2 \chi_c(T) + [\chi_o^{ab} - (g_{ab}/g_c)^2 \chi_o^c].$$

The main point of this analysis is that the fitted slope of the data in Fig. 2 corresponds to the ratio  $(g_{ab}/g_c)^2$ . This ratio is plotted as a function of  $x$  in the inset of Fig. 2. The sample with  $x = 0.67$  has the largest anisotropy of  $g_{ab}/g_c \sim 1.45$ , whereas the sample with  $x = 0.3$  is nearly isotropic. This behavior further highlights the unusual metallic state which exists in the phase diagram for  $x > 0.5$ .

The samples with  $x > 0.5$  can be further analyzed by fitting the high-temperature susceptibility to a Curie-Weiss law,  $\chi = \chi_o + C/T$ . The fits were performed over the range  $T = 50 - 250$  K, and the fit parameters for both field orientations, as well as the powder average, are shown in Table 1. For comparison purposes, results from data taken on a flux-grown crystal with  $x = 0.7$  is also shown. We find that the results of the fits have a small dependence on the choice of the temperature range selected. Overall, however, the fits appear to converge with an error less than 15%. The temperature-independent value for  $\chi_o$  agrees well with the estimate of the orbital contribution ( $\sim 2 \cdot 10^{-4}$  cm<sup>3</sup>/mole) from Knight shift analysis of <sup>59</sup>Co NMR.<sup>12</sup>

The fitted values for the powder average of the single crystal with  $x = 0.75$  yield a Curie constant of  $C \sim 0.147$  K-cm<sup>3</sup>/mole,  $\chi_o \sim 2 \cdot 10^{-4}$  cm<sup>3</sup>/mole, and Weiss temperature  $\theta \sim -125$  K. We have examined the validity of these results for the single crystal sample by mea-

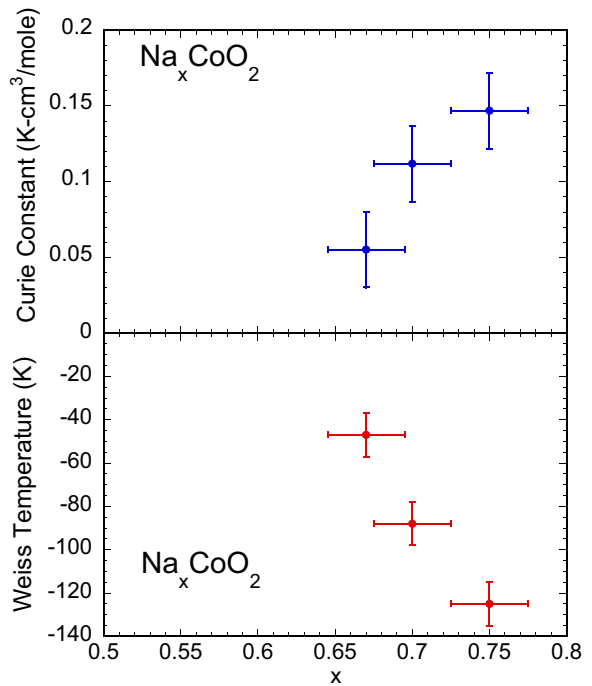


FIG. 3: (color online) Top panel: Curie constant versus  $x$ . Bottom panel: the Weiss temperature versus  $x$ . Both are taken from powder averaged values shown in Table I

suring five different batches of powder  $\text{Na}_{0.75}\text{CoO}_2$  samples (not shown). All Curie constants fall reliably near  $0.149 \pm 0.025$  K-cm<sup>3</sup>/mole. As expected, we find that the Curie constants for  $H \parallel c$  and  $H \parallel ab$  are significantly different for the crystal sample. This may arise from an anisotropic  $g$ -factor as discussed above. In addition, it is likely that part of the axial variation of  $\chi$  results from spin anisotropy of the localized  $\text{Co}^{4+}$  moment.

The effective moment of the  $\text{Co}^{4+}$  ion can be calculated from the powder averaged Curie constant. If we assume that the Curie-Weiss behavior originates from the formal  $1 - x$  fraction of  $\text{Co}^{4+}$  moments with  $S = 1/2$ , then the effective moment  $\mu_{eff} = g\sqrt{S(S+1)}\mu_B \simeq 2.2 \mu_B$  and  $g \simeq 2.5$  for the  $x = 0.75$  sample. This value for the powder averaged  $g$ -factor, where  $g^2 = (2/3 * g_{ab}^2 + 1/3 * g_c^2)$ , can be used to estimate  $g_c$  and  $g_{ab}$  using our data for  $\chi_{ab}(T)/\chi_c(T)$ . We obtain the values  $g_{ab} \simeq 2.7$  and  $g_c \simeq 2.0$ . Alternatively, the value of the Curie constant is consistent with an interpretation in which the effective local moment is  $\sim 1.1 \mu_B$  averaged over all of the Co ions. In either interpretation, the coexistence of localized spins and metallic behavior in this compound remains an intriguing issue to understand.

The results of our fits to the Curie-Weiss law are summarized in Fig. 3. The Curie constant decreases precipitously with decreasing  $x$ . This implies that while almost all of the  $\text{Co}^{4+}$  spins are localized for  $x = 0.75$  (assuming the value  $g \simeq 2.5$  from above), the fraction of localized spins drops sharply as the Na content is reduced. Local moment behavior disappears almost entirely for  $x = 0.5$ .

In parallel with the loss of local moments, the magnitude of the Weiss temperature decreases drastically with decreasing  $x$ . The Weiss temperature of about -125 K for  $x = 0.75$  suggests antiferromagnetic (AF) correlations between  $\text{Co}^{4+}$  spins. There is a clear reduction in the strength of the AF correlations as  $x$  decreases towards  $x = 0.5$ . These results demonstrate that de-intercalating Na from  $\text{Na}_{0.75}\text{CoO}_2$  modifies the spin system from one described by localized spins to one described by delocalized spins with weaker magnetic coupling.

We find the susceptibilities of the two samples with  $x = 0.3$  and  $x = 0.5$  are almost identical (within the errors) above  $\sim 100$  K as shown in Fig. 1, similar to that reported previously in powder samples.<sup>4</sup> Interestingly, we find that our non-hydrated  $\text{Na}_{0.3}\text{CoO}_2$  sample develops small anomalies near  $T = 53$  K and  $T = 88$  K, after the crystal was stored in air for more than 6 months. This suggests that some degree of Na phase separation may occur over long time scales. In our  $\text{Na}_{0.5}\text{CoO}_2$  sample, the susceptibility cusp at  $T \simeq 53$  K is nearly isotropic, whereas the one near  $T \simeq 88$  K is clearly anisotropic.

## 2. Magnetic susceptibility of $\text{Na}_{0.3}\text{CoO}_2 \cdot y\text{H}_2\text{O}$

The magnetic susceptibilities of single crystal samples of  $\text{Na}_{0.3}\text{CoO}_2 \cdot y\text{H}_2\text{O}$  (with  $y \simeq 0, 0.6, 1.3$ ) are shown in Fig. 4. These data were taken on a single sample which originally had the composition  $\text{Na}_{0.3}\text{CoO}_2 \cdot 1.3\text{H}_2\text{O}$  and was subsequently annealed to reduce the water content to  $y = 0.6$  and then  $y = 0$ . All three samples show nearly temperature-independent susceptibilities with weak Curie-Weiss-like behavior developing below  $\sim 200$  K. As water is driven out, the anisotropy of the susceptibility is reduced, and, at the same time, the Curie behavior above 50 K becomes slightly enhanced. In addition, the fully dehydrated crystal is observed to have a small  $\text{Co}_3\text{O}_4$  impurity phase, likely caused by the dehydration process due to partial decomposition. By fitting the susceptibility above  $T = 50$  K for the fully dehydrated crystal to a Curie law, we find that the Curie constant is isotropic and corresponds to about  $\sim 6\%$  isolated  $\text{Co}^{4+}$  ions. We can therefore identify this as an impurity contribution, and this term has been subtracted from the data in the bottom panel of Fig. 4. The Curie corrected susceptibility data for this fully dehydrated  $\text{Na}_{0.3}\text{CoO}_2$  crystal are very similar to the data for the non-hydrated  $\text{Na}_{0.3}\text{CoO}_2$  crystal shown in Fig. 1 (which do not require this correction). There is a cusp in the susceptibility near  $T \sim 42$  K for both the fully hydrated and partially hydrated crystal, which we will discuss further below.

In Fig. 5, we plot  $\chi_{ab}$  versus  $\chi_c$ , which again has a remarkably linear dependence. An anisotropic Curie-Weiss law  $\chi_o + C/(T - \theta)$  has been used to fit both directions. The complete list of fit parameters (above 50K) is shown in Table 2. Both  $C_{ab}/C_c$  and  $(g_{ab}/g_c)^2$  are plotted in the inset of Fig. 5. We find that the ratio  $(g_{ab}/g_c)^2$  is greater than 1 for both the fully hydrated and partially

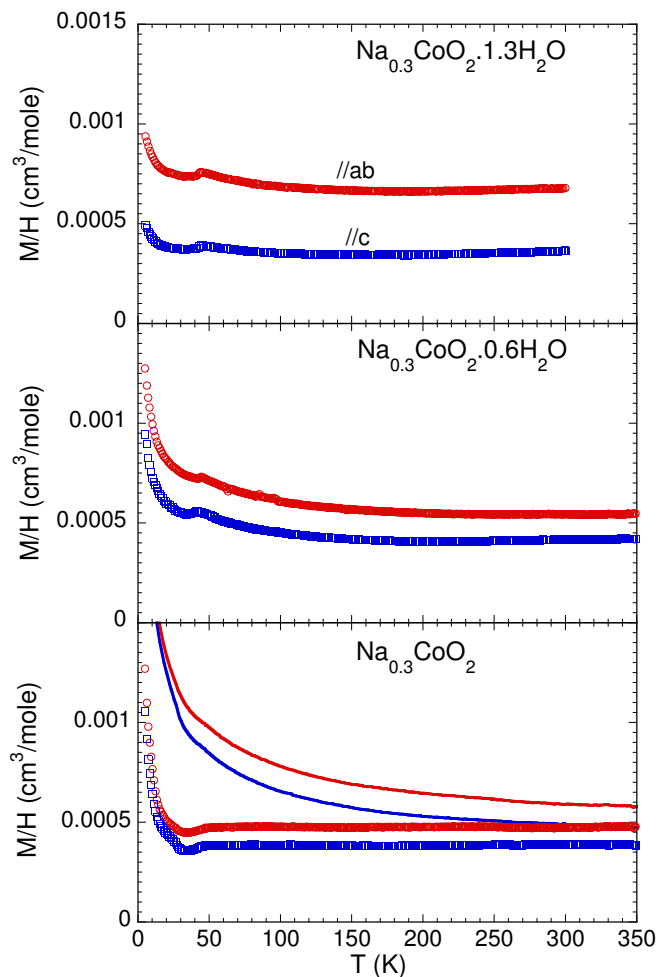


FIG. 4: (color online) Magnetic susceptibilities of  $\text{Na}_{0.3}\text{CoO}_2 \cdot y\text{H}_2\text{O}$  ( $y = 0, 0.6,$  and  $1.3$ ) under a magnetic field of 1 Tesla. The red and blue symbols are for field applied along the  $ab$  and  $c$  directions respectively. The third panel for  $\text{Na}_{0.3}\text{CoO}_2$  shows data both before (lines) and after (symbols) a Curie tail was subtracted.

hydrated samples. This indicates that the paramagnetic moments which give rise to the Curie-Weiss behavior above 50 K are not isotropic, but are strongly affected by the anisotropic orbital environment. Hence, this magnetic signal likely is intrinsic to the crystalline phase. Such Curie-Weiss behavior is absent in the non-hydrated  $\text{Na}_{0.3}\text{CoO}_2$  sample shown previously in Fig. 1. The Curie constant for the fully hydrated  $\text{Na}_{0.3}\text{CoO}_2 \cdot 1.3\text{H}_2\text{O}$  crystal ( $\sim 0.0036$  K-cm<sup>3</sup>/mole) suggests about  $\sim 1\%$  of the spins ( $S = 1/2$  and  $g^2 \sim 6.3$ ) in the system are localized. These localized spins may be related to defects formed during hydration as a result of local structure deformation. However, their origin remains a topic for further investigation. Enhanced Curie-like behavior has been reported in powder samples prepared with the chemical  $\text{Br}_2$  de-intercalation method by Sakurai and coworkers.<sup>13</sup> We note that the Curie behavior observed below 30 K in our samples has a similar degree of anisotropy as the high-

TABLE II: Curie-Weiss fitting parameters for  $\text{Na}_{0.3}\text{CoO}_2 \cdot y\text{H}_2\text{O}$

		y=1.3	y=0.6	y=0
ab	$\chi_o$	.000634	.000472	.000476
ab	C	.00474	.0167	.0385
ab	$\theta$	10.2	-20.6	-26.7
c	$\chi_o$	.000334	.000360	.000383
c	C	.00160	.00954	.0327
c	$\theta$	21.2	-4.12	-20.4
Powder	$\chi_o$	.000533	.000444	.000441
Powder	C	.00363	.0119	.0380
Powder	$\theta$	14.0	-5.93	-27.6

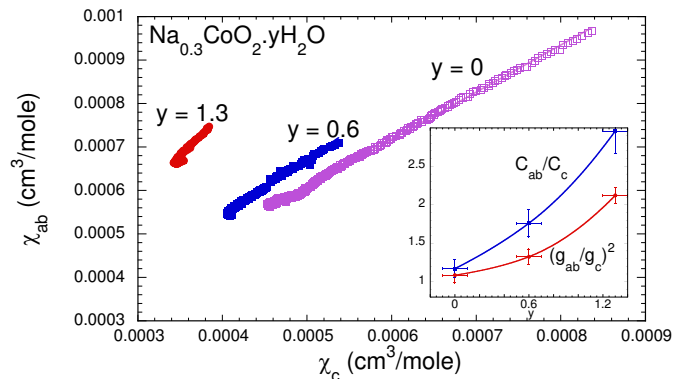


FIG. 5: (color online)  $\chi_{ab}$  versus  $\chi_c$  for  $\text{Na}_{0.3}\text{CoO}_2 \cdot y\text{H}_2\text{O}$  with  $y = 0, 0.6$  and  $1.3$ . The inset shows the fitted slope which corresponds to  $(g_{ab}/g_c)^2$  and Curie constant ratio ( $C_{ab}/C_c$ ) as described in the text. The lines serve as guides for the eye.

temperature susceptibility. Hence, this behavior likely originates from defects intrinsic to the crystalline phase.

Two major differences are made apparent by comparing the susceptibility data of the fully hydrated (FH)  $\text{Na}_{0.3}\text{CoO}_2 \cdot 1.3\text{H}_2\text{O}$  and non-hydrated  $\text{Na}_{0.3}\text{CoO}_2$  crystals displayed in Fig. 1 and Fig. 4. First, the FH sample has a larger anisotropy. Second, the FH sample has a larger total susceptibility. The larger anisotropy likely results from the structural changes of the CoO layers caused by the hydration. The higher susceptibility may result from a change in  $\chi_{vv}$  or  $\chi_{pauli}$ , although we cannot separate these two contributions independently. We note that NMR measurements show that the  $^{59}\text{Co}$  Knight shift is significantly enhanced upon hydration,<sup>12</sup> consistent with our findings. If the susceptibility increase is dominated by  $\chi_{vv}$ , a smaller  $t_{2g}$  splitting would indicate a less distorted  $\text{CoO}_6$  octahedra. However, the neutron powder results of Lynn *et al.* indicate that a fully hydrated sample actually has a larger octahedral distortion compared with a non-hydrated one.<sup>14</sup> On the other hand, if  $\chi_{pauli}$  is dominant, this implies that the fully hydrated sample has a higher density of states at the Fermi level.

#### IV. DISCUSSION AND CONCLUSIONS

In the cuprate superconductors, it is generally found that  $g_c$  is larger than  $g_{ab}$ .<sup>15,16</sup> We find that  $\text{Na}_x\text{CoO}_2 \cdot 1.3\text{H}_2\text{O}$  has the opposite relation  $(g_{ab}/g_c) > 1$ . A significant difference between these families of materials is the orientation of the oxygen octahedra around the Cu and Co ions. In  $\text{La}_2\text{CuO}_4$ , for example, the octahedral Cu-O axes are nearly parallel with the tetragonal crystallographic axes. On the other hand, in  $\text{Na}_x\text{CoO}_2 \cdot y\text{H}_2\text{O}$ , the  $z$ -axis of the crystal field (in Co-O coordinates) is tilted away from the crystallographic  $c$ -direction by nearly  $\sim 60^\circ$ . In addition, the  $\text{CoO}_6$  octahedra are distorted (compressed along the (111) direction in Co-O coordinates) from the ideal configuration.<sup>14,17</sup>

The  $g$ -tensor can be calculated from  $g_{\mu\nu} = 2(\delta_{\mu\nu} - \lambda\Lambda_{\mu\nu})$ , where  $\lambda$  is the spin-orbit coupling constant and  $\Lambda_{\mu\nu} = \sum_n \frac{\langle 0|L_\mu|n\rangle\langle n|L_\nu|0\rangle}{E_n - E_0}$ .<sup>18</sup> In a simple ionic picture, each  $\text{Co}^{4+}$  ion is in the low-spin state with an unpaired electron in the  $a_{1g}$  orbital, higher in energy than the  $E_g$  doublet by an amount  $\Delta$ .<sup>19</sup> In order to calculate the  $g$ -tensor with respect to the crystallographic axes, the orbital wave functions can be transformed from the original Co-O coordinates within the  $\text{CoO}_6$  octahedra to the crystal coordinates in the following way<sup>20</sup>  $|a_{1g}\rangle = d_{3z^2-r^2}$ ,  $|E_{1g}\rangle = (\sqrt{2}d_{xy} + d_{yz})/\sqrt{3}$ , and  $|E_{2g}\rangle = (-\sqrt{2}d_{x^2-y^2} + d_{xz})/\sqrt{3}$ . Using this, we find that  $g_c = 2$ , independent of the  $\lambda/\Delta$  ratio. This is consistent with our estimate of  $g_c$  from the analysis of our susceptibility data. The values for  $g_a$  and  $g_b$  are expected to be larger than 2 so long as  $\lambda$  is negative. We note that this model neglects effects due to hybridization, which may be significant.<sup>21</sup> Recent local density approximation (LDA) calculations by Marianetti and coworkers<sup>21</sup> show that electrons in the  $t_{2g}$  orbitals are accompanied by a redistribution of the charge in the hybridized  $e_g$  and oxygen orbitals.

We remark further on the 42 K anomaly observed in both fully hydrated  $\text{Na}_{0.3}\text{CoO}_2 \cdot 1.3\text{H}_2\text{O}$  and partially hydrated  $\text{Na}_{0.3}\text{CoO}_2 \cdot 0.6\text{H}_2\text{O}$  crystals (shown previously in Fig. 4). This anomaly is much weaker or absent in the fully dehydrated and non-hydrated  $\text{Na}_{0.3}\text{CoO}_2$  crystals. Hence, we conclude that the anomaly results from the hydration process. However, it is not clear at this point if this reflects the intrinsic behavior of the hydrated sample, or if it originates from an impurity phase. We note that the 42 K anomaly does not exist in fully hydrated powder samples, irrespective of chemical or electrochemical de-intercalation. It is therefore tempting to assign the 42 K anomaly to the existence of a  $\text{Co}_3\text{O}_4$  impurity, especially since the bulk AF transition temperature of  $\text{Co}_3\text{O}_4$  occurs around  $\sim 33$  K. However, hysteretic behavior is observed near 42 K (not shown), which is not expected from a  $\text{Co}_3\text{O}_4$  impurity phase. Sasaki and coworkers have also reported a 42 K anomaly in hydrated single crystal samples.<sup>22</sup> They proposed that it originates from residual oxygen on the surface of the crystal. However, if this is only a surface effect, powder samples should show a more pronounced 42 K anomaly under the same treatment. Unlike studies on  $\text{K}_x\text{CoO}_2$  powder samples, where

a  $\text{Co}_3\text{O}_4$  inclusion can be reliably subtracted from the total susceptibility,<sup>23</sup> we cannot completely eliminate the anomaly near 42 K with a simple subtraction of a  $\text{Co}_3\text{O}_4$  ( $T_N \sim 33\text{K}$ ) impurity phase.

In summary, we have presented a systematic study of the magnetic susceptibility of  $\text{Na}_x\text{CoO}_2 \cdot y\text{H}_2\text{O}$  (with  $0.3 < x < 0.75$  and  $y \sim 0, 0.6$  and  $1.3$ ) using single crystal samples. For non-hydrated samples, we find that the derived anisotropic g-factor ratio ( $g_{ab}/g_c$ ) decreases significantly as the composition is changed from the Curie-Weiss metal with  $x = 0.75$  to the paramagnetic metal with  $x = 0.3$ . We confirm that a model of localized  $\text{Co}^{4+}$  spins describes the spin susceptibility of  $\text{Na}_{0.75}\text{CoO}_2$ . However, the fraction of localized spins decreases precipitously upon de-intercalation. For the composition with  $x=0.3$ , the anisotropy in the susceptibility becomes more pronounced with increasing hydration. In addition, the magnitude of the susceptibility is larger in fully hydrated  $\text{Na}_{0.3}\text{CoO}_2 \cdot 1.3\text{H}_2\text{O}$  than in non-hydrated

$\text{Na}_{0.3}\text{CoO}_2$ . The hydrated crystals also contain a small additional fraction of anisotropic localized spins. These results provide a new piece to the picture of how the spin behavior evolves with changing Na content and water content.

### Acknowledgments

We thank P.A. Lee and T. Imai for many insightful discussions. This work was supported primarily by the MR-SEC Program of the National Science Foundation under award number DMR-02-13282. Y.S.L. also acknowledges support by the National Science Foundation under Grant No. DMR 0239377. J.H.C. was partially supported by Grant No. (R01-2000-000-00029-0) from the Basic Research Program of the Korea Science and Engineering Foundation.

- 
- \* On leave from Physics Department, Pusan National University, Korea.
- <sup>1</sup> K. Takada, H. Sakurai, E. Takayama-Muromachi, F. Izumi, R. Dilanian, and T. Sasaki, *Nature* **422**, 53 (2003).
  - <sup>2</sup> I. Terasaki, Y. Sasago, and K. Uchinokura, *Phys. Rev. B* **56**, R12685 (1997).
  - <sup>3</sup> Y. Wang, N. S. Rogado, R. J. Cava, and N. P. Ong, *Nature* **423**, 425 (2003).
  - <sup>4</sup> M. L. Foo, Y. Wang, S. Watauchi, H. W. Zandbergen, T. He, R. J. Cava, and N. P. Ong, cond-mat/0312174.
  - <sup>5</sup> D. J. Singh, *Phys. Rev. B* **68**, 020503 (2003).
  - <sup>6</sup> F. C. Chou, J. H. Cho, P. A. Lee, E. T. Abel, K. Matan, and Y. S. Lee (2004), to be published in *Phys. Rev. Lett.*
  - <sup>7</sup> F. C. Chou, E. T. Abel, J. H. Cho, and Y. S. Lee, cond-mat/0405158.
  - <sup>8</sup> Q. Huang, B. Khaykovich, F. C. Chou, J. H. Cho, J. W. Lynn, and Y. S. Lee, unpublished.
  - <sup>9</sup> M. L. Foo, R. E. Schaak, V. L. Miller, T. Klimczuk, N. S. Rogado, Y. Wang, C. Craley, H. W. Zandbergen, N. P. Ong, and R. J. Cava, *Sol. St. Comm.* **127**, 33 (2003).
  - <sup>10</sup> D. Prakhakaran, A. T. Boothroyd, R. Coldea, and L. M. Helme, cond-mat/0312493.
  - <sup>11</sup> B. C. Sales, R. Jin, K. A. Affholter, P. Khalifah, G. M. Veith, and D. Mandrus, cond-mat/0402379.
  - <sup>12</sup> T. Imai, F. L. Ning, B. W. Statt, and F. C. Chou, unpublished.
  - <sup>13</sup> H. Sakurai, K. Takada, F. Izumi, D. A. Dilanian, T. Sasaki, and E. Takayama-Muromachi, cond-mat/0310717.
  - <sup>14</sup> J. W. Lynn, Q. Huang, C. M. Brown, V. L. Miller, M. L. Foo, R. E. Schaak, C. Y. Jones, E. A. Mackey, and R. J. Cava, *Phys. Rev. B* **68**, 214516 (2003).
  - <sup>15</sup> D. C. Johnston, T. Matsumoto, Y. Yamaguchi, Y. Hidaka, and T. Murakami, *Electronic Properties and Mechanisms of High Tc Superconductors* (Elsevier Science Publishers, 1992).
  - <sup>16</sup> T. Watanabe, T. Fujii, and A. Matsuda, *Phys. Rev. Lett.* **84**, 5848 (2000).
  - <sup>17</sup> J. D. Jorgensen, M. Avdeev, D. G. Hinks, J. C. Burley, and S. Short, *Phys. Rev. B* **68**, 214517 (2003).
  - <sup>18</sup> R. M. White, *Quantum Theory of Magnetism* (Springer-Verlag, 1983).
  - <sup>19</sup> Q. Wang, D. Lee, and P. A. Lee, cond-mat/0304377.
  - <sup>20</sup> L. J. Zou, J. L. Wang, and Z. Zeng, *Phys. Rev. B* **69**, 132505 (2004).
  - <sup>21</sup> C. A. Marianetti, G. Kotliar, and G. Ceder, *Phys. Rev. Lett.* **92**, 196405 (2004).
  - <sup>22</sup> T. Sasaki, P. Badica, N. Yoneyama, K. Yamada, K. Togano, and N. Kobayashi, cond-mat/0402355.
  - <sup>23</sup> S. Nakamura, J. Ohtake, N. Yonezawa, and S. Iida, *J. Phys. Soc. Jpn.* **65**, 358 (1996).